# $LiNbO_3$/Si-Hybrid Slot-Waveguide Electro-Optic Modulators

I. Tomita*†, K. Debnath*‡, K. Ibukuro*, M. K. Husain*, J. Byers*, Z. Zhang*, and S. Saito§

*Department of Electronics & Computer Science, University of Southampton, SO17 1BJ, UK

†Department of Electrical & Computer Engineering, National Institute of Technology, Gifu College, 2236-2 Kamimakuwa, Motosu, Gifu 501-0495, Japan

‡Electronics & Electrical Communication Engineering, Indian Institute of Technology, Kharagpur, West bengal 721302, India

§Sustainable Electronic Technologies, Department of Electronics & Computer Science, Faculty of Physical Science & Engineering, University of Southampton, SO17 1BJ, UK

E-mail: I.Tomita@soton.ac.uk

*Abstract*—A new $LiNbO_3$/Si-hybrid electro-optic modulator that utilizes a doped-Si slot waveguide is proposed. An excellent performance, i.e., an improvement of two orders of magnitude in $V_\pi L$, is demonstrated via simulations when compared with the performance of the conventional $LiNbO_3$ modulators.

*Keywords*—Electro-optic modulator, $LiNbO_3$, Si, Simulation, Slot waveguide

## I. Introduction

Si photonics is revolutionizing the short-reach transceivers in data centers [1], while legacy $LiNbO_3$ optical modulators are still dominating for the long-distance optical communications. The advantages of Si optical modulators are availabilities of low-cost fabrication processes, low-power consumption, and integration capabilities with various optical Si components, while the disadvantages are the operation speed typically up to 40-50Gbps and absence of intrinsic electro-optic (E/O) effect for low-optical-loss operation. Although the conventional $LiNbO_3$ optical modulators have advantages of strong E/O effect without carrier injections, high-speed operation exceeding 100Gbps, and high reliability over other materials, e.g., organic polymers [2], they have disadvantages of lack of patterning processes [3], large feature size (as large as ∼50mm in length), large power consumption due to 50-Ω termination for the travelling-waveguide electrodes, and difficulties of integration.

Here, we report an excellent modulator performance using a type of $LiNbO_3$/Si-hybrid E/O modulator, as shown in Fig. 1, by overcoming those drawbacks of the conventional $LiNbO_3$ modulator with the help of the Si technology.

## II. Device Structure and Function

In the proposed hybrid modulator, doped-Si on top of a silicon-on-insulator (SOI) wafer is patterned into

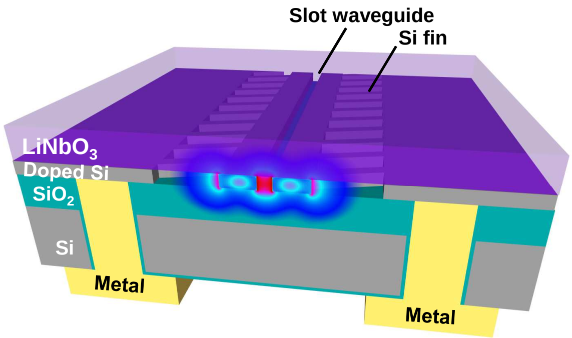


Fig. 1 $LiNbO_3$/Si-hybrid electro-optic modulator. The doped-Si slot waveguide is sandwiched between $LiNbO_3$ and $SiO_2$ layers.

the slot waveguide, and pristine $LiNbO_3$ is bonded onto it (e.g., via the direct-wafer-bonding technique), thus avoiding the difficulties in patterning on $LiNbO_3$. Here we use an evanescent mode [4] formed between the doped-Si slot waveguide and the attached $LiNbO_3$, which gives a small optical core size (or high optical intensity) in $LiNbO_3$. The doped-Si slot waveguide also works as electrodes, which give high electric field to $LiNbO_3$ with small-gapped electrodes. Those features make it possible to remarkably downsize the $LiNbO_3$ modulator of length ∼50mm and core size 3-10$\mu$m, thus achieving low-power consumption by removal of the 50-Ω termination resistor and use of lumped constant circuits. Furthermore, if we can reduce the operation voltage down to 1V with the small-gapped electrodes, we can use a CMOS driver.

Employing the doped-Si slot waveguide with the above excellent properties, our new $LiNbO_3$/Si-hybrid modulator realizes a remarkable improvement in modulator performance (i.e., two orders of magnitude small $V_\pi L$) when compared with the performance of the conventional $LiNbO_3$ modulator ($V_\pi L \sim 10$V·cm [5]), which will be shown in detail in the next section.

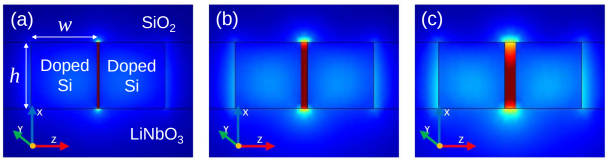


Fig. 2 Optical field of the doped-Si slot waveguide on $LiNbO_3$ at an input wavelength of 1550nm for TE-modes with different slot air-gap sizes: (a) 10 nm, (b) 30 nm, (c) 50 nm. The colors (blue, yellow, red) of the field strength represent $0, 80, 140$V/m, respectively.

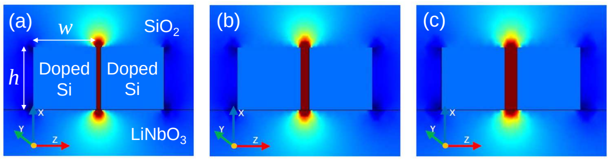


Fig. 3 Electric field ($E_z$) of the horizontal ($z$) direction for the slot waveguide on $LiNbO_3$ with different slot air-gap sizes: (a) 20 nm, (b) 40 nm, (c) 60 nm. The colors (blue, yellow, red) of the field strength represent $0, 2, 5 \times 10^7$V/m, respectively.

## III. Results

Figures 2 and 3 show the computed optical and electric fields for $p$-doped-slot waveguides (doping concentration $1.0 \times 10^{18}$/cm$^3$) with a size of $h = w = 300$nm. We can see evanescent optical and electric field modes in $LiNbO_3$ just under the slot gap, where the top and down layers in Fig. 1 were flipped upside down, and the Si fin structure in Fig. 1 was replaced with a uniform structure with a low refractive index for calculation simplicity. Varying $h$, we observed that at $h < 140$ nm, the optical evanescent mode turned into a perfectly-leaky mode in $LiNbO_3$, thus setting $h = 200$ nm in what follows. The voltage $V_{\rm op}$ applied to the slot gap in Fig. 3 was tentatively set at 5V, but this could be reduced to 1V, while the electric-field pattern is almost unchanged (except for its amplitude).

As the slot gap size $d$ decreases, the spread and intensity of the optical field in $LiNbO_3$ become small, as shown in Fig. 2, although the electric field in Fig. 3 becomes strong because of $E_z = V_{\rm op}/d$. Thus there would be an appropriate $d$ so that it could give the maximum overlap integral between the optical and electric fields (or the maximum modulator performance), which is actually realized at $d = 50$ nm. In this situation, we plotted the half-wavelength voltage $V_\pi$ as a function of the modulator length $L$ (see Fig. 4), where free-carrier optical loss was taken into account. The inset of Fig. 4 shows the logarithmic plot of $V_\pi$ and $L$, which exhibits linearity, thus providing $V_\pi = A/L$, where $A = 416$V$\cdot\mu$m. This means that if we take $V_\pi = 1$V, then $L = 416\mu$m (this small $L$ allows us to use lumped constant circuits, excluding travelling-type resistors). If we change the unit V$\cdot\mu$m to V$\cdot$cm, then we have

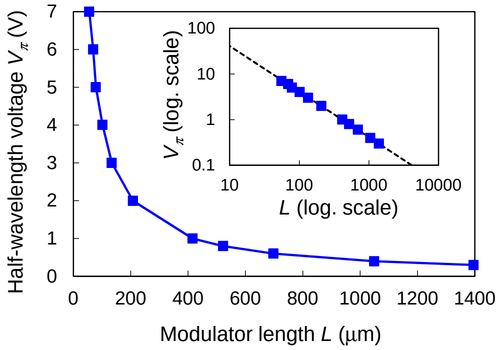


Fig. 4 The half-wavelength voltage $V_\pi$ vs modulator length $L$. The inset shows the logarithmic plot of $V_\pi$ and $L$.

$V_\pi \cdot L = 4.16 \times 10^{-2}$V$\cdot$cm, which is a 1/240 smaller value than that of the conventional $LiNbO_3$ modulator. We also computed $V_\pi \cdot L$ of a $LiNbO_3$/Si-hybrid modulator of a standard waveguide without a slot, and obtained $V_\pi \cdot L = 11.1$V$\cdot$cm as a structure-optimized value, which is a comparable value to the conventional $LiNbO_3$ modulator. In comparison with them, we could confirm the effectiveness of using the doped-Si slot waveguide in the $LiNbO_3$/Si-hybrid modulator.

## IV. Summary

We have examined the performance of a $LiNbO_3$/Si-hybrid E/O modulator with a doped-Si slot waveguide. We have confirmed an excellent performance, i.e., an improvement of two orders of magnitude in $V_\pi L$, when compared with that of the conventional $LiNbO_3$ modulator and the $LiNbO_3$/Si-hybrid modulator with a standard waveguide.

## Acknowledgment

I.T. would like to thank Koshiyama Science & Technology Foundation. S.S. would like to thank EPSRC Manufacturing Fellowship (EP/M008975/1), EPSRC Platform Grant under Grant EP/N013247/1, and the University of Southampton Zepler Institute Research Collaboration Stimulus Fund [6].

## References

[1] G. T. Reed, *Silicon Photonics: The State of the Art*, 1st ed. (John-Wiley & Sons, NJ, 2008).
[2] R. Palmer, L. Alloatti, D. Korn, P. C. Schindler, M. Baier, J. Bolten, T. Wahlbrink, M. Waldow, R. Dinu, W. Freude, C. Koos, and J. Leuthold, IEEE Photon. Tech. Lett. **25**, pp. 1226-1229 (2013).
[3] Z. Ren, P. J. Heard, J. M. Marshall, P. A. Thomas, and S. Yu, J. Appl. Phys. **103**, 034109 (8 pages) (2008).
[4] P. O. Weigel, M. Savanier, C. T. DeRose, A. T. Pomerene, A. L. Starbuck, A. L. Lentine, V. Stenger, and S. Mookherjea, Sci. Rep. **6**, 22301 (9 pages) (2016).
[5] O. Mitomi, K. Noguchi, and H. Miyazawa, IEE Proc. Optoeletron. **145**, pp. 360-364 (1998).
[6] The data from the paper can be obtained from the University of Southampton ePrint research repository: http://doi.org/XXX.